

## Algorithm for Recognition of Left Atrial Appendage Boundaries in Echocardiographic Images

Hossein Ghayoumi Zadeh <sup>1,2\*</sup>, Ali Fayazi <sup>1,2</sup>, Narbeh Melikian <sup>3</sup>, Mark J Monaghan <sup>4</sup>, Mehdi Eskandari <sup>5</sup>

1. Non-communicable Diseases Research Center, Rafsanjan University of Medical Sciences, Rafsanjan, Iran
2. Department of Electrical Engineering, Vali-e-Asr University of Rafsanjan, Rafsanjan, Iran
3. MD, MRCP, King's College Hospital, London, United Kingdom
4. FBSE, FACC, FESC, King's College Hospital, London, United Kingdom
5. MD, FRACP, King's College Hospital, London, United Kingdom

### ARTICLE INFO

**Article type:**  
Original Paper

**Article history:**  
Received: Oct 11, 2019  
Accepted: Jan 31, 2020

**Keywords:**  
Artificial Intelligence  
Atrial Fibrillation  
Computer Vision  
Echocardiographic  
Left Atrial Appendage

### ABSTRACT

**Introduction:** The left atrial appendage (LAA) occlusion using a purpose-built device is a growing procedure. This study aimed to develop a computer-aided diagnostic system for the recognition of the LAA in echocardiographic images.

**Material and Methods:** The three-dimensional (3D) echocardiographic images of the LAA of 26 patients successfully treated with an LAA occluder were used in this study. A total of 208 3D derived two-dimensional images in the axial plane were derived from each 3D dataset. Then, 562 images in which the LAA boundaries were highly recognizable were selected for this study. The proposed convolutional neural network (CNN) in this study was based on open-source object identification and classification platform compiled under the You Only Look Once algorithm. Finally, 419 and 143 images were used for training and testing the algorithm, respectively.

**Results:** Algorithm performance on the identification of the LAA region on a set of 143 images was compared to that reported for the traced regions on the same images by an expert in echocardiography using an intersection over the union (IOU) algorithm. The algorithm was able to correctly identify the LAA region in all 143 examined images with an average IOU of 90.7%.

**Conclusion:** The proposed image-based CNN algorithm in this study showed high accuracy in the recognition of the LAA boundaries in the echocardiographic images. The method can be used in the development of algorithms for the automated analysis of the area of the LAA used for device sizing and procedural planning in the LAA occlusion procedures.

### ► Please cite this article as:

Ghayoumi Zadeh H, Fayazi A, Melikian N, Monaghan M, Eskandari M. Algorithm for Recognition of Left Atrial Appendage Boundaries in Echocardiographic Images. Iran J Med Phys 2021; 18: 123-132. 10.22038/ijmp.2020.43736.1663.

### Introduction

Atrial fibrillation (AF) is the most prevalent cardiac rhythm disturbance. The number of individuals suffering from AF worldwide was about 33.5 million in 2010, with 20.9 and 12.6 million men and women, respectively. The incidence and prevalence rates of AF are even higher in developed countries [1]. However, the growth rate of AF varies among different studies, the incidence of AF was estimated to be doubled in the United States by 2030 [2]. The AF can result in a disabling stroke through clot formation primarily in the left atrial appendage (LAA) and accounts for approximately 20% of the ischemic strokes [3].

The standard treatment for the patients with AF and at risk of stroke is oral anticoagulation agents. However, anticoagulation therapy is associated with the risk of bleeding and contraindicated in the subjects with a history of major bleeding. An alternative treatment in this group of patients is the occlusion of the LAA using a purpose-built device to

prevent the embolization of the clot to the cerebrovascular system [4]. There are currently two main LAA occlusion devices, namely Watchman™ and Amplatzer Amulet™ [5].

The LAA anatomy varies significantly, with an often-elliptical ostium and neck. A careful assessment of the anatomy of the LAA is pivotal in planning for the LAA closure. A crucial step in the planning is determining the size of the device derived from the analysis of a plane below the ostium of the LAA, as the so-called landing zone. Transesophageal echocardiography (TEE) is the imaging modality of choice in many centers for procedural planning and device sizing. Conventionally, the landing zone is measured in multiple two-dimensional (2D) imaging angles; however, owing to the inherent limitations of 2D echocardiography, the chosen plane is not necessarily reflective of the largest and shortest dimensions of the landing zone. Accordingly, there has been a growing interest in the application of three-

dimensional (3D) imaging modalities, namely 3D TEE or multislice computed tomography (MSCT), in the LAA occlusion planning [6,7].

In case of using 3D TEE, a zoomed 3D dataset of the entire LAA and preferably adjacent anatomical landmarks, such as mitral and pulmonary valves, are acquired. By the application of the multiplanar reconstruction technique making it possible to derive 2D images from the 3D dataset, the landing zone is determined as a line drawn at the level of the left circumflex artery to 10-15 mm below the ridge in between pulmonary vein and LAA [7]. Perimeter, shortest, and longest dimensions of the landing zone is then manually measured (Figure 1). These measurements will be taken into account for device sizing based on manufacturer recommendations.

However, the manual identification and analysis of the LAA landing zone is time-consuming and subject to interobserver and intraobserver variability and might lead to device resizing during the procedure which adds to the cost of an already expensive procedure. There has been a growing interest in performing imaging studies to improve the process of image interpretation using automated models. Nevertheless, there is a paucity of the studies in the field of echocardiographic imaging of the LAA in this regard.

For the development of an automated model, the first step is the process of segmentation isolating the boundaries of an image in the form of multiple segments based on its properties, including color,

intensity, and texture of the image. The crucial factors in image segmentation are the dynamic changes of colors, shapes, textures, and scales of images [8]. In general, image segmentation techniques fall into one of the two approaches, namely discontinuities and similarities [9]. In the former approach, the subdivision of images is carried out based on an abrupt change in the intensity of the grey levels of an image; however, in the latter, similarities in the intensity of the grey levels are used to partition an image into the similar regions according to a set of predefined criteria. Edge detection algorithms are the examples of discontinuities approach, and the algorithms, such as thresholding, region growing, region splitting, and merging are based on the similarities approach.

A limited number of studies have been carried out on LAA segmentation techniques only one of which is based on echocardiographic images. A semi-automated algorithm was presented [10] for the LAA segmentation using a region growing algorithm. In another study [11], a fully automatic LAA segmentation method was proposed by an actor-critic reinforcement learning agent. According to the literature [12], a technique based on the fusion of temporal-spatial information was developed for the LAA segmentation and quantitative assisted diagnosis of AF. Wang et al. [13] proposed a semi-automated LAA segmentation technique based on MSCT images that involves four manually selected seed points to obtain the region of interest or bounding box for the LAA.

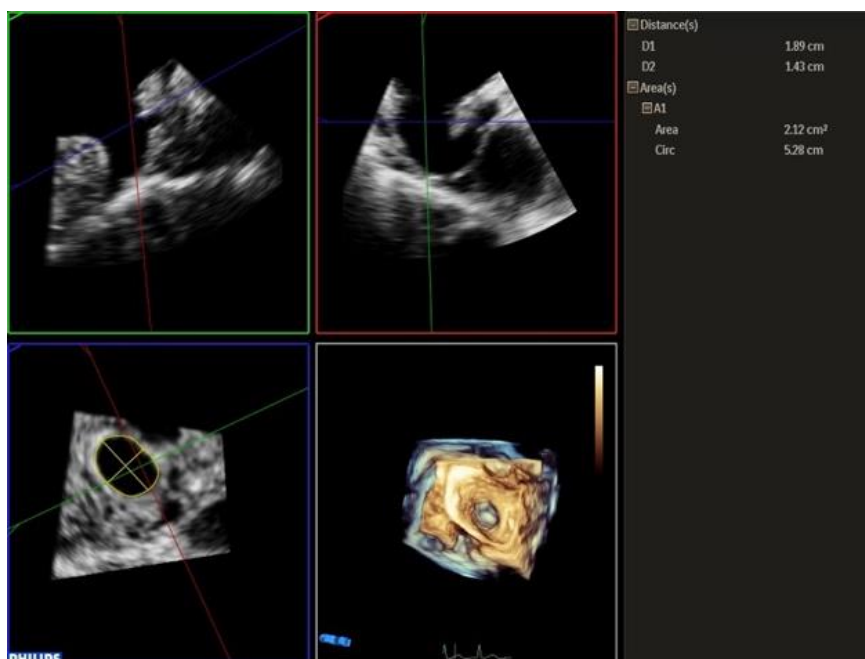


Figure 1. Illustration of multiplanar reconstruction of zoomed three-dimensional echo dataset; green, red, and blue boxes/lines corresponding to sagittal, coronal, and axial (transverse) views; adjustment of blue plane at level of landing zone in sagittal and coronal views (i.e., upper green and red boxes) after alignment of green and red planes; illustration of landing zone in axial (i.e., transverse) plane (i.e., blue box, yellow circle); performing relevant measurements on landing zone

Recently, artificial intelligence (AI) has been used to improve the process of image acquisition and interpretation for the improvement of patient outcomes. The application of learning machines, a subfield of AI, in echocardiography has become an attractive tool to teach echocardiography machines to analyze a vast number of data points using complex computation and statistical algorithms.

However, to the best of our knowledge, there have been a limited number of studies carried out on the use of machine learning in the LAA segmentation arena. Based on the evidence [15], the combination of fully CNNs and modified 3D conditional random fields was used as a robust method utilized to perform the automatic segmentation of the LAA from MSCT data. With this background in mind, the present study proposed an AI-based algorithm for the LAA segmentation and image recognition based on 3D derived 2D echocardiographic images.

## Materials and Methods

### Dataset

The data used in this study were the 3D echocardiographic images of 26 unselected patients who successfully underwent the LAA closure at King's College Hospital London, United Kingdom. The data were prepared according to the standards of the European General Data Protection Regulation, ethical standards of the Institutional and/or National Research Committee (Approval ID in Iran: IR.RUMS.REC.1398.041), as well as 1964 Helsinki Declaration and its later amendments or comparable ethical standards. In addition, the data were completely anonymous and untraceable. The images were obtained by an Epiq 7XT (Philips company, Best, Netherland) echocardiography machine using X7-2t or X8-2t probes (Philips, Best, and Netherland) in a zoomed 3D mode.

### Preprocessing

The first and only preprocessing step in this method was to derive 2D axial images from the 3D zoomed dataset. As illustrated in Figure 1, the landing zone lies in the axial axis of the LAA. For this purpose, an open-source software platform 3D slicer (Harvard University, version 4.11, United States) was used that returns 208 3D derived 2D axial images with the dimensions of 112×128 pixels from a zoomed 3D dataset of the LAA. In the next step, the axial images (i.e., 5408 slices from 26 cases) were examined by an expert in echocardiography, and the LAA border (i.e., the region of interest for the training of the neural network) was traced where feasible.

A total of 562 highly recognizable and traceable axial images were selected out of which 419 and 143 images were used for training the neural network and testing the model, respectively. An example of a patient's slices is shown in Figure 2. As illustrated in the figure, in some slices ( $n=181, 200$ ), the area of the LAA is not properly distinguishable. Therefore, such images were not included in the training process.

### Segmentation

The convolutional neural network (CNN) algorithm for detecting and tracking the LAA presented in this study was based on the identification and classification platform of open-source object compiled under the You Only Look Once (YOLO) algorithm [16]. An image-based CNN was used over a conventional feature-based algorithm. In a featured-based system, the number of determined features, as well as their impact on the diagnostic power of the system, is of paramount importance. Some features are implicitly correlated with each other and can create unnecessary complexity in problem-solving (i.e., overfitting).

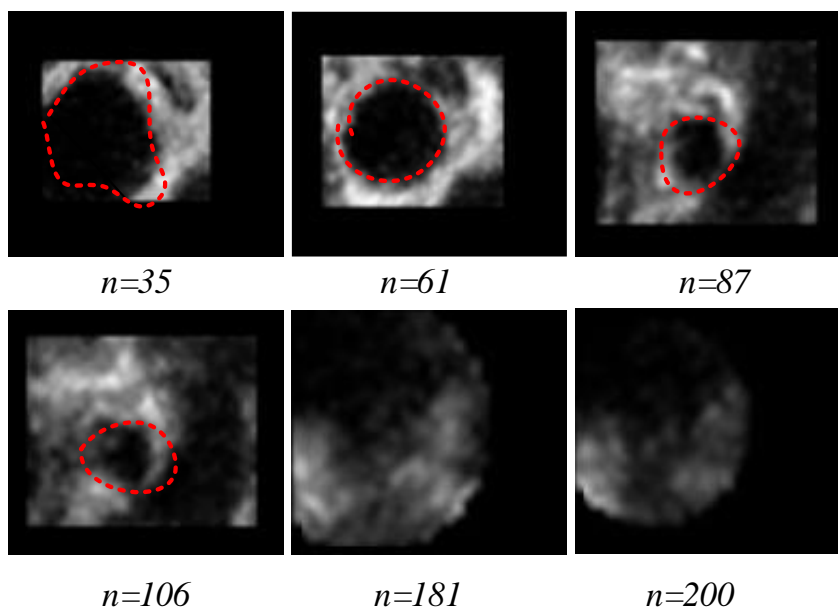


Figure 2. Example of left atrial appendage axial images derived from zoomed three-dimensional echo datasets; no identification of left atrial appendage boundaries in image numbers 181 and 200 leading to exclusion of these images for training of neural network

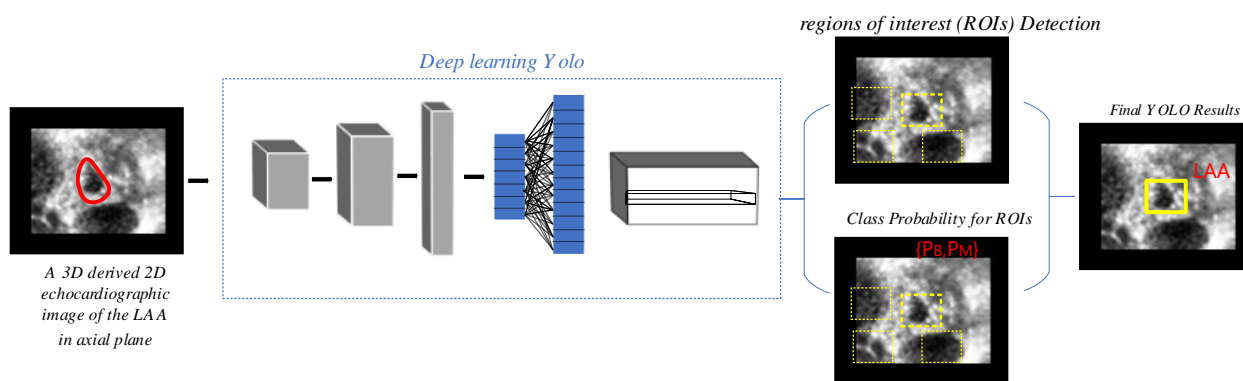


Figure 3. Proposed computer-aided detection and diagnosis system for detecting and tracking left atrial appendage using You Only Look Once model; convolutional neural network, including 24 sets of convolutional layers and 2 fully connected layers to identify left atrial appendage region, as structure of proposed model

In feature-driven neural networks, it is evident that any deficiencies or redundancies in feature extraction or neural network structure design greatly affect the performance of the nervous system in terms of the accuracy and sensitivity of the intelligent system performance.

The segmentation technique used in this study is based on the YOLO model. The YOLO-based computer-aided detection (CAD) and diagnosis system has many advantages over other conventional CNNs. For instance, in many CNNs, the potential bounding boxes in images are suggested by the regional proposal methods. This is pursued by the bounding boxes classification and postprocessing applied to refine the bounding boxes and eliminate the duplicate detections. Finally, all bounding boxes are rescored and reevaluated based on other objects in the scene.

One problem with the above-mentioned methods is that they are used in various locations and scales. It is considered that the high scoring regions are detected from an image and repeated to reach a certain detection threshold. Although these algorithms are precise and used in many application programs, their computations are expensive and almost impossible to be optimized or parallelized which makes them unattractive for the LAA region separation. In addition, in the YOLO-base method, a single neural network is only utilized to split an image into regions and predict bounding boxes and probabilities for each region which is the main advantage of the YOLO-based method.

The proposed YOLO-based CAD system is illustrated in Figure 3. The YOLO network structure is very simple. As depicted in Figure 3, the input resized image is received only by a single convolutional network. Multiple bounding boxes and class probabilities for those boxes are then simultaneously predicted by the single convolutional network. The YOLO trains on full images and directly optimizes detection performance.

It includes a CNN with 24 convolutional layers for feature extraction followed by 2 fully connected layers to predict the probability and coordinates of the objects. In this study, the coordinates of the objects were the LAA regions. Object-detection in the YOLO-based method was accomplished as a tensor-regression problem in which the process started by importing an image into the network. All images were initially resized to  $128 \times 128$  before putting them into the network. A cubic grid sized ( $S \times S$ ) was then superimposed over the image, effectively dividing it into the number of cells ( $n$ ) (Figure 4a). It should be noted that the value of  $S$  should be selected so that it is divisible by image size ( $128 \times 128$ ). If the  $S$  size is set to large, the segmented region will be combined with other regions. Moreover, if it is set to small, the convolution calculation process will be much longer. Bounding boxes ( $B$ ) and confidence scores for those boxes were predicted by each grid cell (Figure 4b).

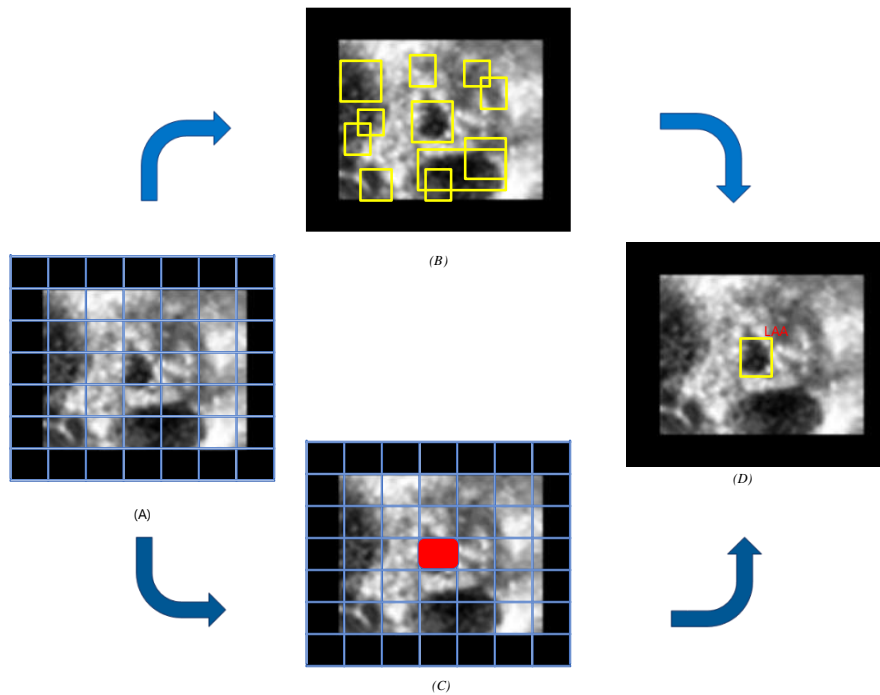


Figure 4. Captured image from a video slide of echocardiographic (A) divided into cells using an equally sized grid (B, C) to uncover key features (D); example of network designed with grid size (S=7) and number of cells (n=49)

The following information can be introduced for each bounding box:

- the box’s center coordinates  $x$  and  $y$  of the bounding box which represent the center of the bounding box relative to the bounds of the grid cell as shown in Figure 4c

- the width ( $w$ ) and height ( $h$ ) of the bounding box predicted relative to the whole image

- the probability of the bounding box composed of the object of interest as a conditional class probability:  $P_r(\text{object})$

The ultimate output layer of the network was reshaped to form an  $S \times S \times (B \times 5 + C)$  tensor, where  $C$  denotes the number of classes, and  $B$  is the number of hypothetical object bounding boxes. Nonmaximal suppression method was applied to remove duplicate detections. A loss function should be used subsequently. This function changed the weights of the grid so that the boundary selected by the neural network was more consistent with the boundary labeled by the specialist physician resulting in lower errors and more reliability. During the training stage, the network loss function was used as it follows [17]:

$$\lambda_{coord} \sum_{i=0}^{S^2} \sum_{j=0}^B 1_{ij}^{obj} (\sqrt{w_i} - \sqrt{\hat{w}_i})^2 + (\sqrt{h_i} - \sqrt{\hat{h}_i})^2 \quad (1)$$

where  $\lambda_{coord}$  is the weight assigned to the loss over the coordinates;  $w_i$  is the width of the bounding box;  $h_i$  is the height of the bounding box, and  $1_{ij}^{obj}$  is the function that counts if the  $j$ th bounding box predictor in cell  $i$  is responsible for the prediction of the object. As described in the preceding text, the coordinates  $w$  and  $h$  correspond to the width and height of the box,

respectively. At each run, the network output was checked by the loss function criterion. If the separated region was not similar to the desired region, the values of the convolution filters were changed to minimize the error criterion, and the values of  $w$  and  $h$  were most consistent with the region of interest.

In this paper, a 24 convolutional layers YOLO network was used for the detection task followed by 2 fully connected layers. This network structure impressively reduced computational time but at the expense of marginally decreasing the classification accuracy of object detection. Table 1 tabulates the full 26-layer network structure. The details of network architecture and network training process are described in the literature [17].

Algorithm performance on identifying the LAA region on the set of 143 images was compared to that reported for the traced regions on the same images by an expert in echocardiography using the intersection over the union (IOU) ratio that assessed the similarity between the grand truth and automatic segmentation. The ratio is calculated as it follows [17]:

$$IOU = \frac{|V_{seg} \cap V_{gt}|}{|V_{seg} \cup V_{gt}|} \quad (2)$$

where  $V_{gt}$  and  $V_{seg}$  denote the volume of the ground truth and automatic segmentation, respectively. As much as the two ratios are closer to 1, the automatic results are closer to the manual.

Table 1. Configuration of You Only Look Once deep neural network structure to track left atrial appendage

Name	Type	Activations	Learnable	Total Learnables
Input 128×128×1 images	Image input	128×128×1	-	0
Conv_1 16 3×3×1 convolutions	Convolution	128×128×16	Weight 3×3×1×16 Bias 1×1×16	160
BN1 (16 channels)	Batch normalization	128×128×16	Offset 1×1×16 Scale 1×1×16	32
Relu_1	Relu	128×128×16	-	0
MaxPool1 2×2	Max pooling	64×64×32	-	0
Conv_2 32 3×3×16 convolutions	Convolution	64×64×32	Weight 3×3×16×32 Bias 1×1×32	4640
BN2 (32 channels)	Batch normalization	64×64×32	Offset 1×1×32 Scale 1×1×32	64
Relu_2	Relu	64×64×32	-	0
MaxPool2 2×2	Max Pooling	32×32×32	-	0
Conv_3 64 3×3×32 convolutions	Convolution	32×32×64	Weight 3×3×32×64 Bias 1×1×64	18496
BN3 (64 channels)	Batch normalization	32×32×64	Offset 1×1×64 Scale 1×1×64	128
Relu_3	Relu	32×32×64	-	0
MaxPool3 2×2	Max pooling	16×16×128	-	0
Conv_4 128 3×3×64 convolutions	Convolution	16×16×128	Weight 3×3×64×128 Bias 1×1×128	73856
BN4 (128 channels)	Batch normalization	16×16×128	Offset 1×1×128 Scale 1×1×128	256
Relu_4	Relu	16×16×128	-	0
Yolov2Conv1 128 3×3×128 convolutions	Convolution	16×16×128	Weight 3×3×128×128 Bias 1×1×128	147584
Yolov2Batch1 (128 channels)	Batch normalization	16×16×128	Offset 1×1×128 Scale 1×1×128	256
Yolov2Relu1 Relu	Relu	16×16×128	-	0
Yolov2Conv2 128 3×3×128 convolutions	Convolution	16×16×128	Weight 3×3×128×128 Bias 1×1×128	147584
Yolov2Batch2 (128 channels)	Batch normalization	16×16×128	Offset 1×1×128 Scale 1×1×128	256
Yolov2Relu2 Relu	Relu	16×16×128	-	0
Yolov2ClassConv 24 1×1×128 convolutions	Convolution	16×16×24	Weight 1×1×128×24 Bias 1×1×24	3096
Yolov2Transform Yolo v2 Transform layer with 4 anchors	Yolo* v2 transform layer	16×16×24	-	0
Yolov2Outputlayer Yolo v2 output with 4 anchors	Yolo v2 output	-	-	0

Yolo: You Only Look Once

## Results

The best results were obtained when mini-batch size, epoch, initial learn rate, learning rate, and iteration number were 8, 50, 0.001, 0.0001, and 4300, respectively. The remaining 143 images were used for

testing CNN recognition accuracy. Two of the various scenarios of the obtained results are shown in Figure 5. Notably in all scenarios, the region of interest (i.e., the LAA border) was correctly detected.

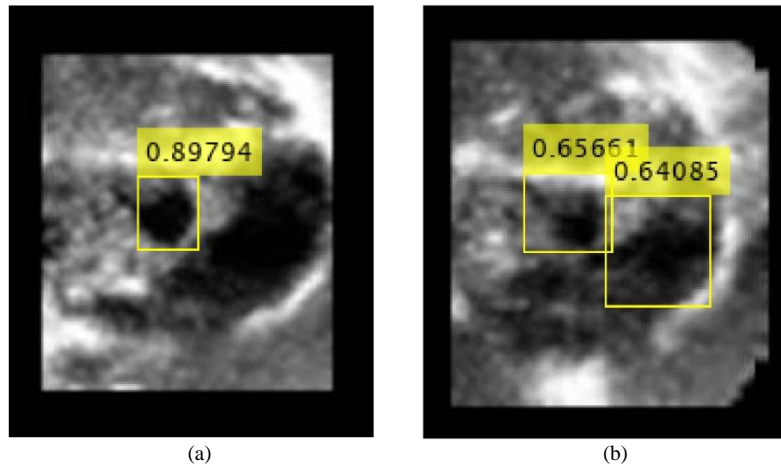


Figure 5. Types of obtained results from proposed network; (a) correct identification of left atrial appendage region by network; (b) consideration of two regions as left atrial appendage region by network

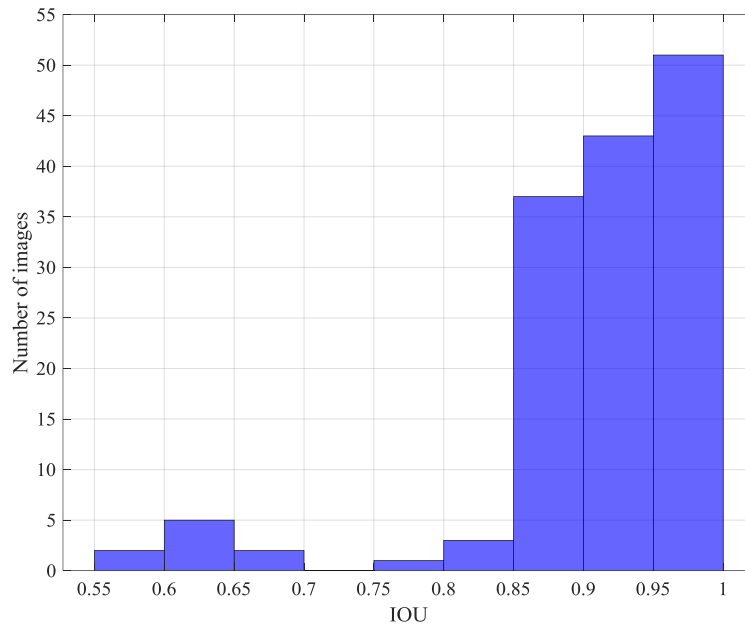


Figure 6. Levels of intersection over the union (IOU) in identification of left atrial appendage by proposed method

Figure 6 depicts the IOU of the 143 images. Notably, the algorithm was able to correctly identify the LAA region in all 143 examined images with an average IOU of 90.7%.

An example of the segmented images is illustrated in Figure 7. As it can be observed, in most images, the

deep neural network was able to identify the LAA region with a high rate of probability. In cases where the region has not been fully assigned or dropped in the image, this identification has been made less accurately, as illustrated in Figure 7c.

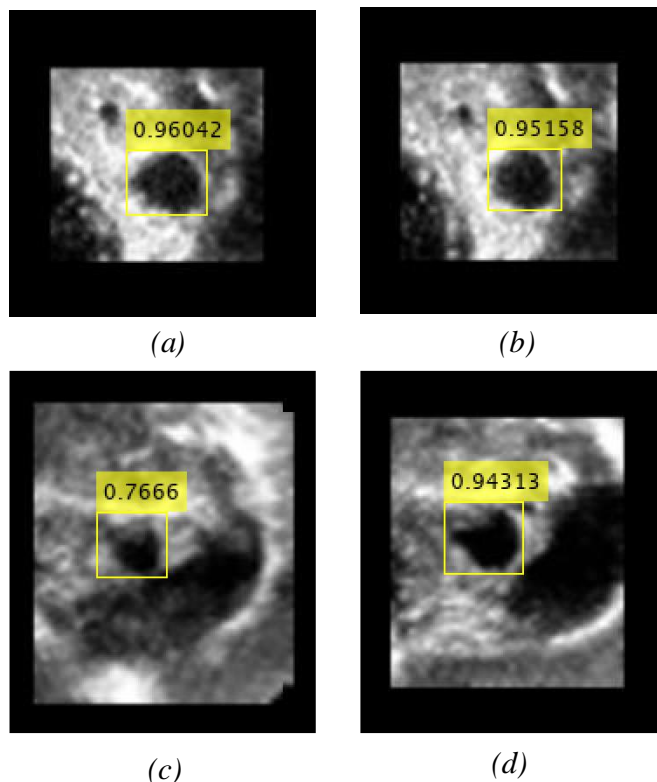


Figure 7. Example of segmented images of left atrial appendage region by You Only Look Once algorithm

### Discussion

In this study, a YOLO-based CAD algorithm was proposed for tracking and recognizing the LAA region on 3D derived 2D axial images that can be used for the development of a model for the automated recognition and analysis of the LAA landing zone. An essential step in planning the LAA closure is the manual identification of the LAA landing zone and measurement of its longest and shortest dimensions and perimeter (Figure 1). The application of learning machines-based algorithms in echocardiography is in its infancy. Within different subtypes of machine learning, the application of CNN in echocardiography has been only reported in the recognition of views obtained by echocardiography and quantification of wall motion abnormalities [14].

The CNN appears to be an attractive approach for the development of algorithms for automated tracking and recognizing the LAA landing zone from 3D derived 2D images. There are several localized CNNs, such as RCNN(Region Based Convolutional Neural Networks), RPN(Region Proposal Network), Fast R-CNN, and YOLO, that can be used for this purpose [18]. Fast R-CNN offers a classification at the rate of one frame per 2

sec that is 25 times faster than the R-CNN approach [19]. Simonyan and Zisserman proposed very deep convolution networks of up to 19 weight layers. The application of the proposed 16-weight layer by Simonyan and Zisserman in Faster R-CNN improved the rate to 7 frames/sec, outperforming the R-CNN by 200 times.

However, the YOLO based algorithms used in the current study remain the fastest algorithms for the recognition of machine vision. The advantage of the image-based intelligent structure used in the present study is no requirement of manual feature extraction as it is designed to learn and identify the intended purpose and automatically extracting the required features. The RCNN and Fast R-CNN algorithms were also trained with a similar set of 526 images and tested with the 143 images. The average rates of IOU were 93.97% and 84.52% for RCNN and Fast R-CNN, respectively. The LAA border detection in the 143 images was successful in only 36 and 57 images by the RCNN and Fast-RCNN, respectively (Figure 8).

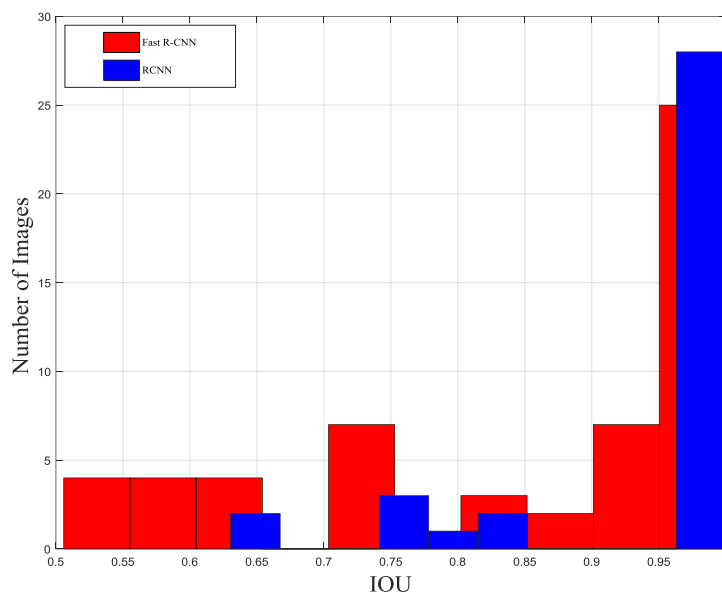


Figure 8. Comparison of intersection over the union (IOU) levels in identification of left atrial appendage by (Region Based Convolutional Neural Networks) RCNN and Fast R-CNN neural networks

Although the majority of previous studies on the identification of the LAA region have been carried out based on different CT images [12, 20, 21] and also the quality of CT images is much higher than echocardiographic images, The advantage of the proposed method is that it is able to perform well in the field of intelligent segmentation. Another contribution of the present study was the use of 2D images for segmentation. The vast majority of previous studies have been conducted using 3D images with their difficulties.

## Conclusion

In this study, an image-based CNN algorithm was developed for the detection of the LAA boundary from 3D derived 2D echocardiographic images. This potentially could help develop an algorithm for the automated detection and analysis of the LAA landing zone for planning and device sizing of the LAA occlusion.

## Acknowledgment

This study was made possible by the financial support of Non-communicable Diseases Research Center of Rafsanjan University of Medical Sciences (grant no: 98003). Also, we express our deep thanks to King's College Hospital of London for their technical support from us.

## References

1. Kirchhof P, Bernussi S, Kotecha D, Heidbuchel H. ESC guidelines for the management of atrial fibrillation developed in collaboration with EACTS. *Revista española de cardiología-Madrid*. 2017;70(1):1-84.
2. Colilla S, Crow A, Petkun W, Singer DE, Simon T, Liu X. Estimates of current and future incidence and prevalence of atrial fibrillation in the US adult population. *The American journal of cardiology*. 2013;112(8):1142-7.
3. Sposato LA, Cipriano LE, Saposnik G, Ruiz Vargas E, Riccio PM, Hachinski V. Diagnosis of atrial fibrillation after stroke and transient ischaemic attack: a systematic review and meta-analysis. *Lancet Neurol*. 2015;14(4):377-87.
4. Kirchhof P, Benussi S, Kotecha D, Ahlsson A, Atar D, Casadei B, et al. 2016 ESC Guidelines for the management of atrial fibrillation developed in collaboration with EACTS. *Eur Heart J*. 2016;37(38):2893-962.
5. Asmarats L, Rodes-Cabau J. Percutaneous Left Atrial Appendage Closure: Current Devices and Clinical Outcomes. *Circ Cardiovasc Interv*. 2017;10(11).
6. Cabrera JA, Saremi F, Sanchez-Quintana D. Left atrial appendage: anatomy and imaging landmarks pertinent to percutaneous transcatheter occlusion. *Heart*. 2014;100(20):1636-50.
7. Wunderlich NC, Beigel R, Swaans MJ, Ho SY, Siegel RJ. Percutaneous interventions for left atrial appendage exclusion: options, assessment, and imaging using 2D and 3D echocardiography. *JACC Cardiovasc Imaging*. 2015;8(4):472-88.
8. Acharya J, Gadhiya S, Raviya K. Segmentation techniques for image analysis: A review. *International Journal of computer science and management research*. 2013;2(1):1218-21.
9. Sivakumar P, Meenakshi S. A review on image segmentation techniques. *International Journal of Advanced Research in Computer Engineering & Technology (IJARCET)*. 2016;5(3):641-7.
10. Leventic H, Babin D, Velicki L, Devos D, Galic I, Zlokolica V, et al. Left atrial appendage segmentation from 3D CCTA images for occluder placement procedure. *Comput Biol Med*. 2019;104:163-74.
11. Al WA, Yun ID. Actor-Critic Reinforcement Learning for Automatic Left Atrial Appendage

- Segmentation. 2018 IEEE International Conference on Bioinformatics and Biomedicine (BIBM). 2018.
12. Jin C, Feng J, Wang L, Yu H, Liu J, Lu J, et al. Left atrial appendage segmentation and quantitative assisted diagnosis of atrial fibrillation based on fusion of temporal-spatial information. *Computers in biology and medicine*. 2018;96:52-68.
  13. Wang L, Feng J, Jin C, Lu J, Zhou J. Left atrial appendage segmentation based on ranking 2-D segmentation proposals. *International Workshop on Statistical Atlases and Computational Models of the Heart*; 2016.
  14. Alsharqi M, Woodward WJ, Mumith JA, Markham DC, Upton R, Leeson P. Artificial intelligence and echocardiography. *Echo Res Pract*. 2018;5(4):11-25.
  15. Jin C, Feng J, Wang L, Yu H, Liu J, Lu J, et al. Left atrial appendage segmentation using fully convolutional neural networks and modified three-dimensional conditional random fields. *IEEE journal of biomedical and health informatics*. 2018;22(6):1906-16.
  16. Li J, Su Z, Geng J, Yin Y. Real-time detection of steel strip surface defects based on improved yolo detection network. *IFAC-PapersOnLine*. 2018;51(21):76-81.
  17. Radovic M, Adarkwa O, Wang Q. Object recognition in aerial images using convolutional neural networks. *Journal of Imaging*. 2017;3(2):21.
  18. Wang Q, Rasmussen C, Song C. Fast, Deep Detection and Tracking of Birds and Nests. *International Symposium on Visual Computing*; 2016.
  19. Simonyan K, Zisserman A. Very deep convolutional networks for large-scale image recognition. *arXiv preprint arXiv:14091556*. 2014.
  20. Zheng Y, Yang D, John M, Comaniciu D. Multi-part modeling and segmentation of left atrium in C-arm CT for image-guided ablation of atrial fibrillation. *IEEE transactions on medical imaging*. 2013;33(2):318-31.
  21. Leventić H, Babin D, Velicki L, Devos D, Galić I, Zlokolica V, et al. Left atrial appendage segmentation from 3D CCTA images for occluder placement procedure. *Computers in biology and medicine*. 2019;104:163-74.